Crystalline Self-Assembly into Monolayers of Folded Oligomers at the Air–Water Interface

Kay Lederer,[b] Adelheid Godt,*[b] Paul B. Howes,[c] Kristian Kjaer,[c] Jens Als-Nielsen,[d] Meir Lahav,[a] Gerhard Wegner,[b] Leslie Leiserowitz,*[a] and Isabelle Weissbuch*[a]

Abstract: Insertion of the 1,3-bis(ethynylene)benzene unit as a rigid spacer into a linear alkyl chain, thus separating the two resulting stems by 9 Å, induces chain folding at the air–water interface. These folded molecules self-assemble into crystalline monolayers at this interface, with the plane of the folding unit almost perpendicular to the water surface, as determined by synchrotron grazing-incidence X-ray diffraction. Three distinct molecular shapes, of the types U, inverted U, and M, were obtained in the two-dimensional crystalline state, depending upon the number of spacer units, and the number and position of the hydrophilic groups in the molecule. The molecules form ribbons with a higher crystal coherence in the direction of stacking between the molecular ribbons, and a lower coherence along the ribbon direction. A similar molecule, but with a spacer unit that imposes a 5 Å separation between alkyl chains, yields the conventional herringbone arrangement.

Keywords: bis(alkynyl)benzenes · grazing-incidence X-ray diffraction · monolayers · oligomers · self-assembly

Introduction

Chain folding is an important feature in the crystallization of many natural[1] and synthetic[2, 3] macromolecules. Numerous experiments,[4] as well as molecular dynamics simulations,[5–7] on ethylene oligomers have been carried out to show that chain folding is a function of its length. The required length for folding to occur in such oligomers is about 100 to 150 carbon atoms, depending mainly on the crystallization conditions.[8–11] However, chains of such a length are barely soluble in conventional organic solvents. Our aim was to design sufficiently soluble molecules that can fold and pack into two-dimensional crystals at the air–water interface.[12–16] Monolayers of folded molecules, as an example for supramolecular design, are of interest as model systems for the early stages of molecular self-organization and crystallization, and as model systems for biological membranes.

The central idea of our molecular design was to obtain folded oligomers by linking linear, aliphatic chains of similar or equal length by evenly spaced, rigid structural units that promote chain folding and packing in crystalline monolayers at the air–water interface. We chose 1,3-bis(ethynylene)-benzene (Figure 1) as the rigid spacer unit, because its dimensions, which correspond to an intramolecular separation between the chains of about 9 Å, would preclude van der Waals contacts between them. This separation by 9 Å is approximately twice the normal van der Waals distance between aliphatic chains in crystals, and it would be stabilized by intermolecular contacts leading to the formation of a close-packed crystalline monolayer containing folded molecules. We have previously reported on compound **2a** (Figure 2) that contains the 1,3-bis(ethynylene)benzene unit and self-assembles into crystalline monolayers at the air–water interface by adopting an inverted U shape.[17]

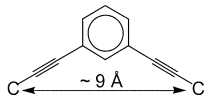

Figure 1. The 1,3-bis(ethynylene)benzene unit.

Here we present the synthesis of a variety of structurally related molecules and the investigation of their two-dimensional crystallization[18, 19] behavior at the air–water interface, to demonstrate the general feasibility of our concept. The crystalline packing arrangements of the Langmuir monolayers

[a] Prof. L. Leiserowitz, Dr. I. Weissbuch, Prof. M. Lahav
Department of Materials and Interfaces
Weizmann Institute of Science, 76100 Rehovot (Israel)
Fax: (+972) 8-934-4138
E-mail: isabelle.weissbuch@weizmann.ac.il

[b] Dr. A. Godt, Dr. K. Lederer, Prof. G. Wegner
Max Planck Institut für Polymerforschung
Ackermannweg 10, 55128 Mainz (Germany)

[c] Dr. P. B. Howes, Dr. K. Kjaer
Physics Department
Risø National Laboratory, 4000 Roskilde (Denmark)

[d] Prof. J. Als-Nielsen
Niels Bohr Institute
H. C. Ørsted Laboratory, 2100 Copenhagen (Denmark)

  0947-6539/00/0612-2173 $ 17.50+.50/0

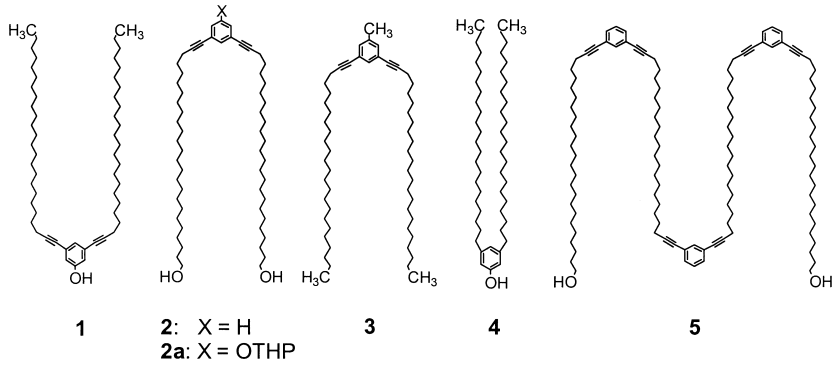

Figure 2. Schematic representation of compounds **1**–**5** in the conformations they adopt at the air–water interface.

were determined by grazing-incidence X-ray diffraction (GIXD) with synchrotron radiation.[20] Additional information on the average thickness of some of the monolayer systems was obtained either by specular X-ray reflectivity measurements[20] or from topography images of the films, transferred onto solid support, by scanning force microscopy (SFM).

Results and Discussion

The five different molecules **1**–**5** investigated in this work are shown schematically in Figure 2. Three of them, **1**, **2** and **3**, have a central 1,3-bis(ethynylene)benzene unit (Figure 1) and differ mainly in the number and position of their polar groups, which can induce favorable interactions with the water subphase. These molecules each have the potential to fold about the 1,3-bis(ethynylene)benzene unit. For comparison with the molecules **1**–**3**, we synthesized and investigated molecule **4** as an example of a conventional two-chain amphiphile,[21] since its central spacer unit, the benzene ring, lacks the two triple bonds. Finally, compound **5** with—potentially—three folds was synthesized according to the molecular design concept of **1**–**3**, and its two-dimensional crystallization behavior at the air–water interface was studied.

Synthesis: The key step in the synthesis of compounds **1**, **2**, **3**, and **5** is an aryl–alkynyl coupling catalyzed by $[Pd(PPh_3)_2Cl_2]$ and CuI.[22] Compound **3** and compounds **8a**–**c**, the precursors for compounds **9a**, **1**, and **2**, respectively (Scheme 1),

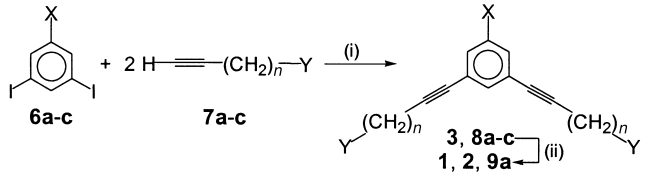

6	X
a	H
b	OTHP
c	CH_3

7	Y	n
a	OTBDMS	19
b	CH_3	21
c	OTBDMS	23

8a → **9a**
8b → **1**
8c → **2**

	X	Y	n
8a	H	OTBDMS	19
8b	OTHP	CH_3	21
8c	H	OTBDMS	23
9a	H	OH	19
1	OH	CH_3	21
2	H	OH	23
3	CH_3	CH_3	21

Scheme 1. i) $[Pd(PPh_3)_2Cl_2]$, CuI, THF, piperidine, RT, 16 h; ii) for **8b**: dioxane, MeOH, TosOH, RT, 1 h; for **8a**, **c**: *n*-$BuNF_4$, THF, RT, 1 h.

were obtained by the coupling of 1,3-diiodobenzenes **6** with 1-alkynes **7**. Subsequent deprotection of the OH groups of the precursors **8a**–**c** yielded the compounds **9a**, **1**, and **2**. Compound **9a** is one of the starting materials for the synthesis of compound **5** (Scheme 2). The α,ω-diol **9a** was transformed into the α,ω-diyne **9c** via the intermediate α,ω-dibromide **9b**. The α,ω-diyne **9c** was coupled with the 3-alkynyliodoben-

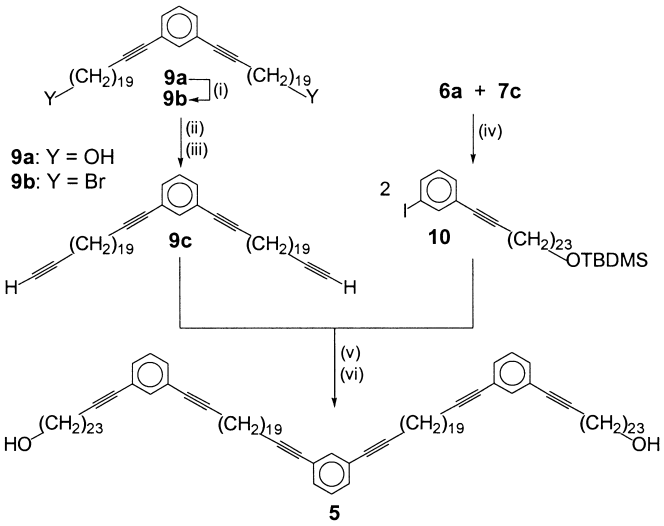

Scheme 2. i) PPh_3, Br_2, imidazole, CH_2Cl_2, RT, 8 h; ii) LiC≡C–TMS, THF, 1,3-dimethyl-3,4,5,6-tetrahydro-2-pyrimidone, RT, 16 h; iii) *n*-$BuNF_4$, THF, 2 h, RT; iv) $[Pd(PPh_3)_2Cl_2]$, CuI, THF, piperidine, RT, 16 h; v) $[Pd(PPh_3)_2Cl_2]$, CuI, THF, piperidine, RT, 16 h; vi) *n*-$BuNF_4$, THF, 1 h, RT.

zene **10** (Scheme 2) to give, after desilylation, compound **5**. Coupling partner **10** was obtained as the main product by the reaction of 1,3-diiodobenzene **6c** with one equivalent of the *O*-protected alkynol **7c** and was easily isolated by column chromatography. Compound **4** was synthesized by a $[Ni(dppp)Cl_2]$-catalyzed coupling reaction of Grignard reagent **12** with the *O*-protected 3,5-dichlorophenol **11**,[23] followed by desilylation of the coupling product (Scheme 3).

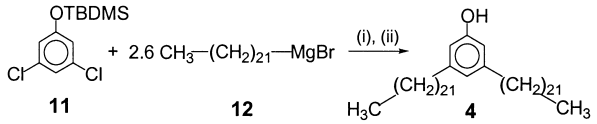

Scheme 3. i) $[Ni(dppp)Cl_2]$, diethyl ether, reflux, 5 days; ii) *n*-$BuNF_4$, THF, 2 h, RT.

Self-assembled crystalline monolayers at the air–water interface: The surface pressure–area (Π–A) isotherms of compounds **1**–**5** are shown in Figure 3. The isotherms of compounds **1**–**4** each display a steep rise in surface pressure

0947-6539/00/0612-2174 $ 17.50+.50/0 *Chem. Eur. J.* **2000**, *6*, No. 12

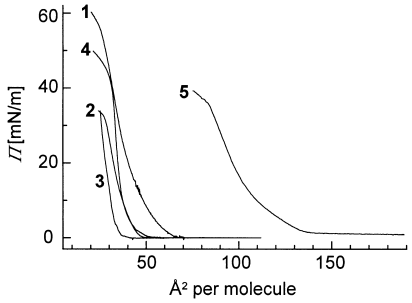

Figure 3. $\Pi - A$ isotherms of compounds **1**–**5** at the air–water interface.

at a nominal molecular area (defined as the Langmuir trough area divided by the number of spread molecules) of 30–50 Å^2. For compound **5**, the surface pressure rises steeply and yields an area per molecule of approximately 80 Å^2. This value already indicates that molecules of **5** self-assemble and adopt a conformation in which the four alkyl chains of one molecule are oriented almost perpendicularly to the water surface.

*Compound **1***: The structure of the film of **1** was characterized by GIXD measurements performed at various points along the isotherm; the measurement started at low monolayer coverage. The GIXD patterns measured at a nominal molecular area of 100 and 50 Å^2 are presented in Figure 4 as

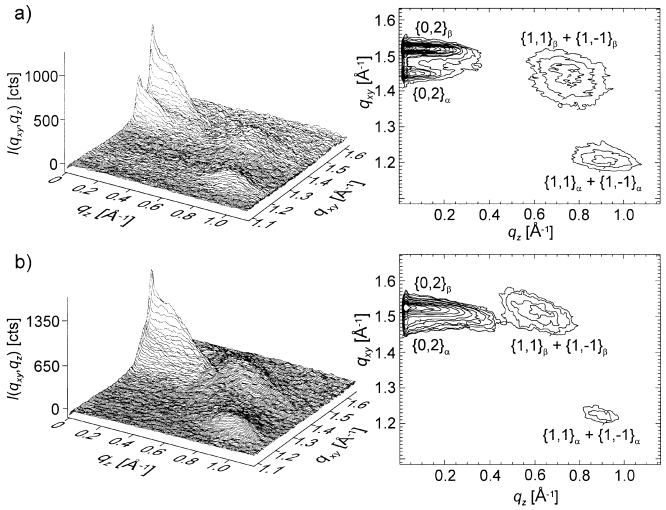

Figure 4. Two-dimensional surface (left) and contour (right) plots of the scattered intensity $I(q_{xy},q_z)$ as a function of the horizontal (q_{xy}) and the vertical (q_z) components of the scattering vector q from a monolayer of compound **1** at nominal molecular areas of: a) 100 Å^2 and b) 50 Å^2.

two-dimensional surface and contour plots of the scattered intensity $I(q_{xz},q_z)$ as a function of both the horizontal (q_{xy}) and the vertical (q_z) components of the scattering vector. We observed that a crystalline monolayer is formed already at a nominal molecular area of 100 Å^2, corresponding to 40% surface coverage, as the four Bragg peaks in Figure 4a show. These Bragg peaks are interpreted in terms of two crystalline phases, α and β. The diffraction peaks are assigned $\{h,k\}$ Miller indices, which yields two rectangular "subcells" (a_s, b_s) that, according to their area, each contain two alkyl chains (Table 1). The main difference between the two crystalline

Table 1. Assignment of the GIXD data measured for the monolayer of compound **1**, calculated unit-cell parameters and crystalline coherence lengths $L_{h,k}$.

$\{h,k\}$ Miller index for subcell[a]	α phase		β phase	
	q_{xy} [Å^{-1}]	$q_{z,max}$ [Å^{-1}]	q_{xy} [Å^{-1}]	$q_{z,max}$ [Å^{-1}]
{0,2}	1.445	0	1.516	0
{1,1}+{1,−1}	1.205	0.90	1.445	0.73
a_s [Å]	6.52		5.11	
b_s [Å]	8.70		8.29	
γ [°]	90		90	
t [°][b]	43 (along a)		30.7 (along a)	
A_{chain} [Å^2][c]	28.4		21.2	
A_{proj} [Å^2][d]	20.7		18.2	
L [Å]	$L_{1,1}=110$, $L_{0,2}=200$		$L_{1,1}=70$, $L_{0,2}=180$	
$a=a_s$ [Å]	6.52		5.11	
$b=2b_s$ [Å]	17.40		16.58	

[a] The calculated parameters a_s, b_s and γ belong to the subcells containing two chains, but not a true unit cell repeat, in view of the molecular structure. The parameters a, b and γ belong to the true unit cell which contain two molecules. [b] t = molecular tilt angle. [c] A_{chain} = area per chain = $0.5a_sb_s$. [d] A_{proj} = projected area per chain = $0.5\,a_pb_p = 0.5\,a_sb_s\cos t$.

phases α and β is in their molecular tilt angles from the surface normal, 43° and 31°, respectively, in the direction of the a_s axis; this was deduced from the q_z maxima of the Bragg rod intensity profiles. We shall present a detailed analysis only of the packing arrangement of the α-phase.

The subcell of the α phase is centered, since the {0,1} and {1,0} reflections were not observed. The length of the b_s axis, which is 8.7 Å, corresponds approximately to the distance between the ends of the two triple bonds in the 1,3-bis(ethynylene)benzene unit (Figure 1), which separates the two chains of the molecule. Thus a molecule is arranged in the subcell of the α-phase with its central spacer unit aligned parallel to the b_s axis at (x,y) positions (0,0) and (0,1) and tilted along the a_s axis (Figure 5a). Therefore, in view of the

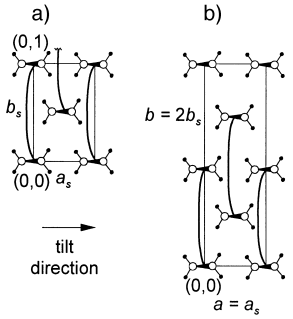

Figure 5. Schematic representation of the packing of molecules of **1** in the crystalline monolayer of the α phase, shown for: a) the subcell and b) the true unit cell.

structural requirement, the b_s axis must be doubled to give the true unit cell repeat as $b=2b_s$ (Figure 5b and Table 1). Along the a_s axis, the unit cell repeat remains unchanged, $a=a_s$. For this ab unit cell, which contains two molecules, the Miller indices of the {0,2} and {1,1}+{1,−1} Bragg peaks must be reassigned to {0,4} and {1,2}+{1,−2}, respectively. Consequently, molecules in adjacent ribbons are placed with their chains at (x,y) positions (0,0) and (0,0.5), and (0.5,0.25) and

(0.5,0.75) as shown in Figure 5b. This arrangement yields intermolecular distances with favorable van der Waals contacts. Structural considerations require positional disorder of adjacent ribbons that may be offset randomly along the b direction by $\pm 0.5b$. In this way, equidistant separation between chains along directions $0.5(a \pm 0.5b)$ can be obtained by virtue of symmetry; this also results directly in the appearance of a rectangular unit cell.

We performed X-ray structure-factor calculations[24] by use of an atomic-coordinate molecular model constructed with the Cerius^2 computer program.[25] Calculations based upon the assumption of an ordered packing arrangement as in Figure 5b yielded relatively strong {0,1} and {1,1}+{1,−1} Bragg rods; the latter do not agree with observation.[26] These calculated intensities can arise only from the contribution of the 1,3-bis(ethynylene)benzene unit in an ordered arrangement. The best fit between the measured and calculated Bragg rod intensity profiles (Figure 6a, b) was obtained for molecules tilted by 45° along the a axis in the packing arrangement shown in Figure 6c–e. For clarity, only the ordered arrangement in the ab unit cell is presented. Note that the calculated Bragg rods of the {0,4} and {1,2}+{1,−2} reflections shown in Figure 6a,b are the same for the ordered and disordered arrangements. We assume that the absolute orientation of the molecule is fixed by the affinity of the hydrophilic OH groups for the water surface,[27] which results in a U-shape molecular conformation of **1**.

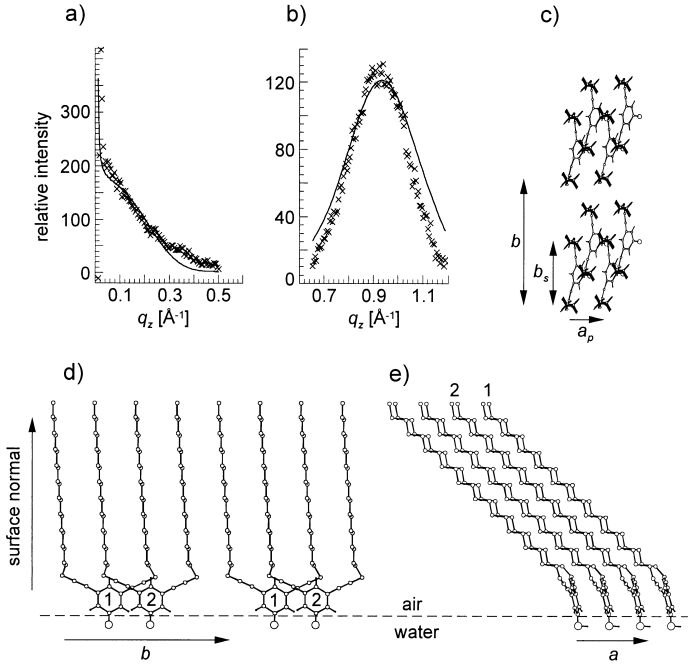

Figure 6. a) and b): Measured (×) and fitted (line) intensity profiles $I(q_z)$ of the two Bragg rods {0,4} and {1,2}+{1,−2} corresponding to the crystalline α phase. c)–e) The two-dimensional packing arrangement of compound **1** in the crystalline α phase viewed along: c) the chain axis, d) the a axis, and e) the b axis. For clarity, hydrogen atoms are omitted in d) and e). Adjacent molecular ribbons are labeled 1 and 2. The unit cell dimensions projected down the chain axis, a_p and b_p, are given by $a_p = a_s \cos t$ and $b_p = b_s$, where t is the chain tilt.

The GIXD pattern obtained from the monolayer compressed to a nominal molecular area of 50 Å^2 (Figure 4b) shows that the {0,2} Bragg peaks of the α and β crystalline phases coalesce, yet the system remains dimorphic, retaining essentially the same packing arrangements.

Compound ***2***: The role played by the position and number of the hydrophilic OH groups was investigated by studying the monolayer of molecule **2**, which is complementary to **1**, since its 1,3-bis(ethynylene)benzene unit is hydrophobic, whereas the chain ends are hydrophilic (Figure 2). We expected molecule **2** to self-assemble into a monolayer by adopting an inverted U-shape, as a result of the affinity of the OH groups for water. Molecule **2** is related to the previously reported[17] inverted U-shape molecule **2a**, but lacks the bulky OTHP group at the spacer unit.

The GIXD pattern measured for **2** spread on water at a nominal molecular area of 100 Å^2 (Figure 7) is very similar to that previously observed for molecule **2a**.[17] For the monolayer of **2**, we found the same dimorphism as for **2a**, that is, coexistence of a rectangular and an oblique two-dimensional subcell (Table 2). The subcell dimensions and the molecular-chain tilt of the two crystalline phases of **2** are very similar to the corresponding phases reported for **2a**, as are, by consequence, their two-dimensional crystalline packing arrangements (Figure 8). These results demonstrate a) the negligible effect of the bulky group OTHP of the spacer unit on the self-assembly of inverted U-shape molecules at the air–water interface and b) the reproducibility of our results.

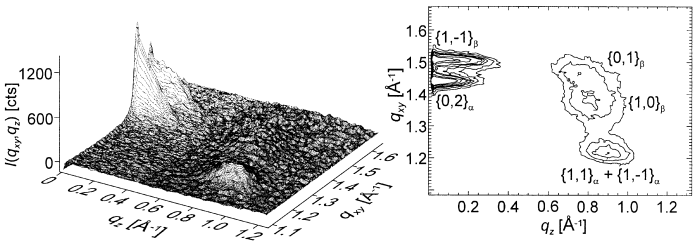

Figure 7. Two-dimensional surface (left) and contour (right) plots of the scattered intensity $I(q_{xy}, q_z)$ from a monolayer of compound **2** at a nominal molecular area of 100 Å^2.

GIXD measurements (not shown) of the monolayer of **2** compressed to a nominal molecular area of 50 Å^2 revealed that the crystalline α-phase remains unchanged, whereas the β-phase underwent a transition from a pseudo-rectangular to a rectangular unit cell of similar dimensions.

Compound ***3***: The question arose whether a molecule linked by the 1,3-bis(ethynylene)benzene spacer unit, such as molecules **1**, **2**, and **2a**, but which lacks hydrophilic groups, would still self-assemble into crystalline monolayers at the air–water interface. For this purpose, compound **3** was synthesized. Indeed, our concept held for compound **3** at low surface coverage (70 Å^2 per molecule, i.e., 55% coverage), according to the GIXD pattern (Figure 9). Only one crystalline phase is formed. The derived subcell dimensions ($a_s = 5.01$ Å, $b_s = 7.57$ Å, $\gamma = 90°$) indicate a herringbone

  0947-6539/00/0612-2176 $ 17.50+.50/0 *Chem. Eur. J.* **2000**, *6*, No. 12

Table 2. Assignment of the GIXD data measured for the monolayer of compound **2**, calculated unit-cell parameters and crystalline coherence lengths $L_{h,k}$.

{*h*,*k*} Miller index of subcell[a]	α phase rectangular subcell		β phase oblique subcell	
	q_{xy} [Å^{-1}]	$q_{z,max}$ [Å^{-1}]	q_{xy} [Å^{-1}]	$q_{z,max}$ [Å^{-1}]
{0,2}	1.440	0.00	–	–
$\{1,1\}+\{1,-1\}_\alpha$	1.220	0.90	–	–
$\{1,-1\}_\beta$	–	–	1.505	0.07
$\{0,1\}_\beta$	–	–	1.480	0.76
$\{1,0\}_\beta$	–	–	1.385	0.82
a_s [Å]	6.38		5.08	
b_s [Å]	8.73		4.75	
γ [°]	90		116.8	
t [°][b]	42 (along a)		33 (along a)	
A_{chain} [Å^2][c]	27.9		21.5	
A_{proj} [Å^2][d]	20.7		18.0	
L [Å]	$L_{1,1}=100$, $L_{0,2}=200$		$L_{1,0}=40$, $L_{0,1}=70$, $L_{1,-1}=160$	
$a=a_s$ [Å]	6.38		5.16[e]	
$b=2b_s$ [Å]	17.46		16.75[e]	
γ [°]	90		96.5[e]	

[a] The calculated parameters a_s, b_s, and γ_s belong to subcells containing two chains but not a true unit cell repeat, in view of the molecular structure. The parameters a, b and γ belong to the true unit cells which contain two molecules. [b] t = tilt angle. [c] A_{chain} = area per chain. [d] A_{proj} = projected area per chain. [e] Note that for the oblique β phase, a_s and b_s were converted into the pseudo-rectangular unit cell dimensions $\boldsymbol{a}=(\boldsymbol{a}_s+\boldsymbol{b}_s)$ and $\boldsymbol{b}=2(\boldsymbol{b}_s-\boldsymbol{a}_s)$.[17]

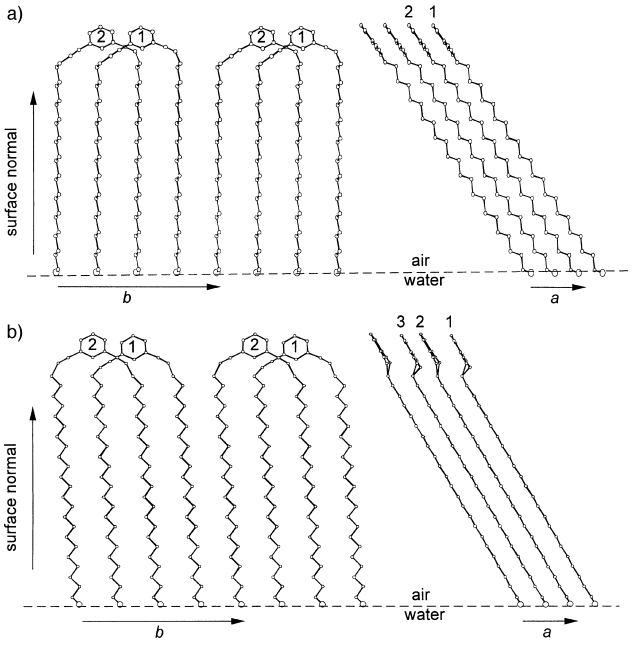

Figure 8. The packing arrangement of compound **2** in the crystalline α- (a) and β (b) phases viewed along the *a* axis (left) and the *b* axis (right).

packing of vertically aligned alkyl chains.[18] The crystalline film thickness, determined from the full width at half maximum (FWHM(q_z)) of the Bragg rod intensity profiles, is about 29 Å, indicative of a monolayer of folded molecules. We may construct the two-dimensional crystalline packing of molecule **3** in three possible ways, shown schematically in Figure 10. The two chains of one molecule are placed at the lattice points (0,0) and (1,1) separated by 9.1 Å, a distance corresponding to the span of the 1,3-bis(ethynylene)benzene

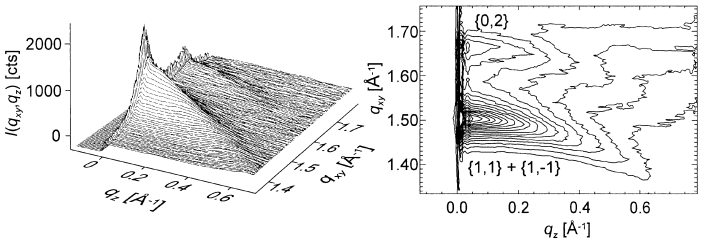

Figure 9. Two-dimensional surface (left) and contour (right) plots of the scattered intensity $I(q_{xy}, q_z)$ from a monolayer of molecules of **3** at a nominal molecular area of 70 Å^2.

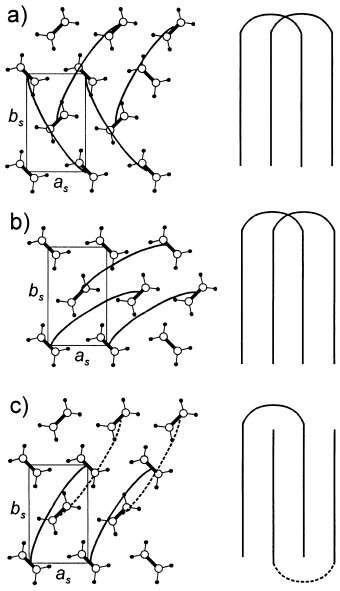

Figure 10. Schematic representation of the three possible ways (a–c) of packing molecules of **3** in the crystalline monolayer with the alkyl chains arranged in a herringbone motif. Top (left) and side (right) views of the molecular chains. The curved line represents the spacer unit.

unit (Figure 10a). This packing arrangement would, in all likelihood, lead to spatial hindrance between the rigid spacer unit and chains of adjacent molecules. Such poor contacts may be circumvented in the arrangement shown in Figure 10b, in which the two chains of a molecule are placed at positions (0,0) and (1.5,0.5). The intramolecular chain–chain distance is 8.4 Å. In principle, we may also consider the formation of an interdigitated arrangement (Figure 10c) in order to avoid the poor contacts of Figure 10a, but this packing is less probable, since it would embody a rougher film–water interface.

Specular X-ray reflectivity measurements of the film at the air–water interface provided additional information on the average film thickness. The calculated reflectivity curve in Figure 11 involved a two-box model based on the molecular structure of **2**—the first box contained the alkyl chains and the second the spacer units—with the parameters shown in Table 3. In the fitting procedure, the number of electrons in each box, calculated from the molecular structure of **2**, the area occupied by the molecule, determined from the GIXD data, and the surface coverage of the monolayer, calculated from the number of molecules spread on the water surface, were kept fixed (Table 3). The length of the two boxes and the

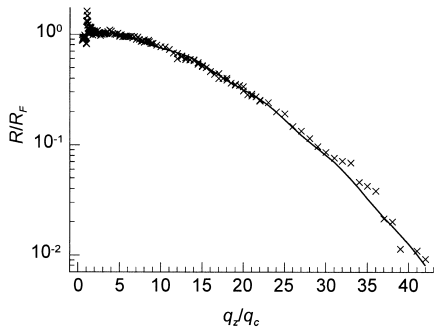

Figure 11. Measured (×) and calculated (line) specular X-ray reflectivity curve for a monolayer of compound **3** at a nominal molecular area of 50 Å^2.

Table 3. Fitted parameters[a] of the two-box model of electron density corresponding to the calculated reflectivity curve for the monolayer of compound **3**.

no. of boxes	% *cov*	*A* [Å^2]	ρ_1/ρ_w [Å]	L_1 [Å]	ρ_2/ρ_W [Å]	L_2 [Å]	L_T	σ
2	80	39.5	1.02	26.3	1.01	5.5	31.8	3.0

[a] % *cov* is the surface coverage of the monolayer; *A* is the area occupied by one molecule; $\rho_W = 0.334$ e Å^{-3} is the electron density of the water subphase; ρ_1 (N_1 is the number of electrons = 354) and ρ_2 ($N_2 = 72$) are the electron densities of boxes 1 and 2 respectively, where $\rho_j = N_j/AL_j$ and L_1, L_2 are the length of the boxes, respectively; the total length is $L_T = L_1 + L_2$; σ is the surface roughness parameter.

surface roughness were refined to the values given in Table 3, so that an average film thickness of about 32 Å was obtained; this value is close to the thickness of the crystalline part of the monolayer determined by GIXD.

On the basis of all the above results, we can dismiss any arrangement in which one of the chains of **3** is closely packed normal to the water surface and the other disordered, with the molecule unfolded.

Compound ***4***: To give an experimental illustration of a molecular fold promoted by a moiety other than the 1,3-bis(ethynylene)benzene unit, we investigated compound **4**. This molecule is structurally derived from **1**, but lacks the two triple bonds attached to the benzene ring that may act as a spacer preventing intramolecular van der Waals contacts between the chains during the self-assembly process. Therefore, the two-dimensional crystallization behavior of molecule **4**, as an example for a conventional two-chain amphiphile, should be different from that of **1** and **2**. The benzene ring of **4** separates the stems of its two alkane chains by approximately 5 Å, a value that is close to the distance between nearest-neighbor chains in *n*-alkane crystals.[28] Consequently, intramolecular van der Waals contacts between the chains should be energetically favored during the self-assembly into two-dimensional crystallites at the air–water interface.

The GIXD pattern measured at a nominal molecular area of 70 Å^2 (Figure 12a) shows the formation of a self-assembled crystalline monolayer at about 62 % surface coverage. The two Bragg peaks are interpreted in terms of a rectangular unit cell (Table 4) with the molecular chains tilted by about 26° with respect to the surface normal. In contrast to all the systems described above, in this crystalline monolayer the molecules are tilted in the direction of the unit cell axis *b*, as

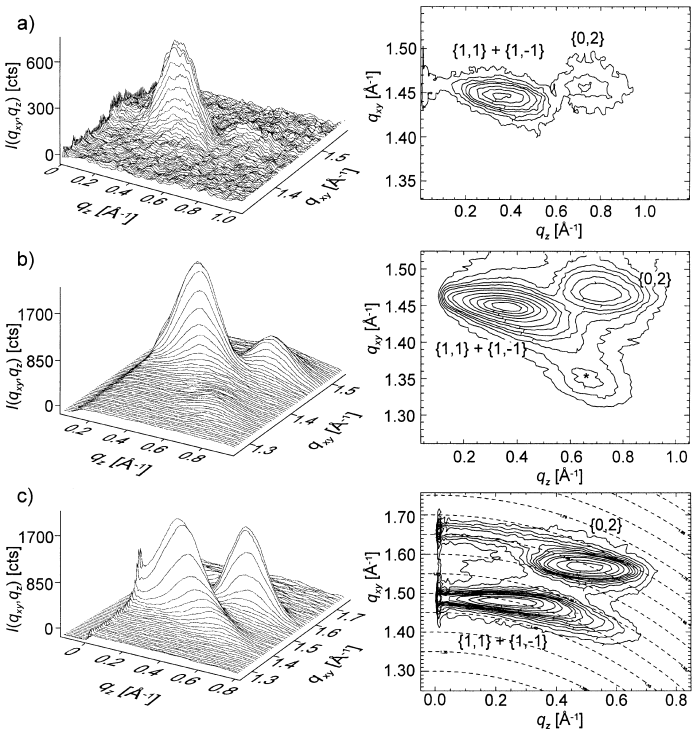

Figure 12. Two-dimensional surface (left) and contour (right) plots of the scattered intensity $I(q_{xy}, q_z)$ from a monolayer of compound **4** at nominal molecular areas of: a) 70 Å^2, b) 50 Å^2, and c) 38 Å^2. The dashed lines in the contour plot of c) represent lines of $q_t = (q_{xy}^2 + q_z^2)^{1/2}$ = constant. Note that the unassigned Bragg peak in b) is marked with an asterisk.

Table 4. Assignment of the GIXD data measured for the monolayer of compound **4** and calculated unit cell parameters of the crystalline α phase.

{*h*,*k*} Miller index	70 Å^2 per molecule		50 Å^2 per molecule		38 Å^2 per molecule	
	q_{xy} [Å^{-1}]	$q_{z,max}$[Å^{-1}]	q_{xy} [Å^{-1}]	$q_{z,max}$[Å^{-1}]	q_{xy} [Å^{-1}]	$q_{z,max}$[Å^{-1}]
{0,2}	1.455	0.74	1.466	0.72	1.570	0.50
{1,1}+{1,−1}	1.445	0.35	1.448	0.36	1.480	0.25
a (a_p) [Å]	5.03 (5.03)		5.03 (5.03)		5.00 (5.00)	
b (b_p) [Å]	8.64 (7.76)		8.57 (7.70)		8.00 (7.61)	
γ [°]	90		90		90	
t [°][a]	26 (along *b*)		26 (along *b*)		18 (along *b*)	
A_{chain} [Å^2][b]	21.73		21.55		20.00	
A_{chain} [Å^2][c]	19.52		19.37		19.05	

[a] *t* = tilt angle. [b] A_{chain} = area per chain. [c] A_{proj} = projected area per chain.

determined from the q_z maxima of the two Bragg rod intensity profiles.

On compression of the film to 50 Å^2 per molecule, the intensity of the two Bragg rods (Figure 12a) increase (Figure 12b); at the same time a weak peak at $q_{xy} = 1.35$ Å^{-1} and $q_z = 0.66$ Å^{-1}, which belongs to an additional crystalline phase, appears.[29] Further compression to 38 Å^2 per molecule yields a GIXD pattern (Figure 12c) in which the two Bragg rods belonging to the initial phase have their q_z maxima at lower q_z values. The unit cell dimensions of this phase decrease slightly, since the molecular chain tilt is reduced by 8° (Table 4). The GIXD pattern in Figure 12c shows additional Bragg peaks at $q_{xy} = 1.49$ Å^{-1} and 1.66 Å^{-1}, $q_z = 0$ Å^{-1}; these are skewed along lines of $q_t = (q_{xy}^2 + q_z^2)^{1/2}$ = constant. These skewed peaks yield a rectangular unit cell of dimensions 5.1 Å × 7.6 Å; this

0947-6539/00/0612-2178 $ 17.50+.50/0 *Chem. Eur. J.* **2000**, *6*, No. 12

corresponds to herringbone packing of vertically aligned alkyl chains. The skewing behavior may be interpreted in terms of monolayer bending, which occurs on compression of the film.[13, 30]

We now discuss the packing arrangement of the self-assembled dominant crystalline phase observed for molecule **4**. The unit cell dimensions (a_p and b_p) of this phase projected down the molecular chain axis are given by $a_p = a$ and $b_p = b\cos t$, for which t is the chain tilt angle with respect to the surface normal. The values of a_p and b_p (Table 4) are almost the same ($a_p = 5.0$ Å and $b_p = 7.7$ Å) for the different compression states of the monolayer and are evidence for a herringbone packing of the alkyl chains. In contrast, the projected unit cells of the crystalline phases of **1** and **2** (e.g., $a_p = a_s\cos t = 4.8$ Å and $b_p = b = 8.7$ Å for the α-phase of **1** in which the chain tilt is along the a axis) are clearly different from that observed for the herringbone motif.

We performed X-ray structure factor computations, using an atomic coordinate model, to fit the Bragg rod intensity profiles of the dominant phase in Figure 12b. The model, which contains chains of 20 CH_2 groups tilted by 27° from the surface normal along the b axis, yielded the calculated Bragg rod intensity profiles shown in Figure 13a and b. However,

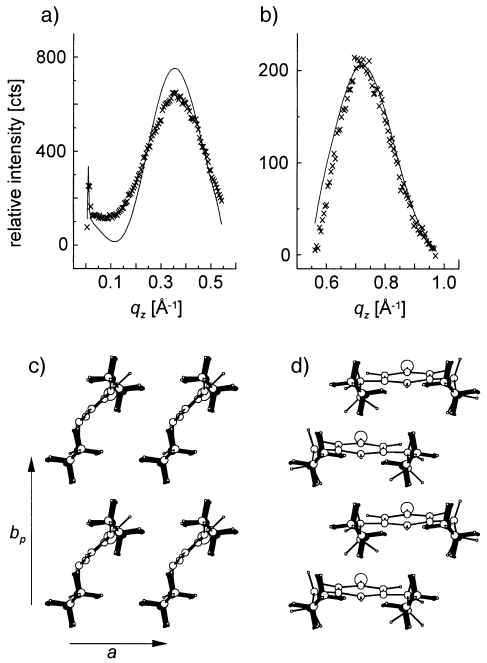

Figure 13. a) Measured (×) and b) calculated (line) intensity profiles of the {0,2} and the {1,1}+{1, – 1} Bragg rods obtained from the monolayer of compound **4**; c) and d): Herringbone packing arrangement depicting the two possible spacer linkages.

there is an ambiguity as to whether the chain linkage is oriented along the a axis (Figure 13d) or along the unit cell diagonal 0.5(***a***+***b***) (Figure 13c). We favor the arrangement in Figure 13d, since the dimensions of the linkage are unaffected by the change in the molecular tilt angle t, which occurs upon film compression (see Table 4). A positional disorder in this molecular packing arrangement is caused by the fact that adjacent molecules along the b direction may be randomly offset by $\pm 0.5\,a$.

Molecule ***5***: Finally, we extended our studies towards an oligomer that can be described as being built up of two inverted U-shape molecules, similar to **2**, linked by the 1,3-bis(ethynylene)benzene spacer unit. This molecule was designed to fold three times into an M-shape, promoted by the affinity of the two hydrophilic OH end groups to water (Figure 2).

Indeed, molecule **5** self-assembles on water at a surface coverage as low as 30% (nominal molecular area of 260 Å^2). The GIXD pattern, shown in Figure 14 for a nominal

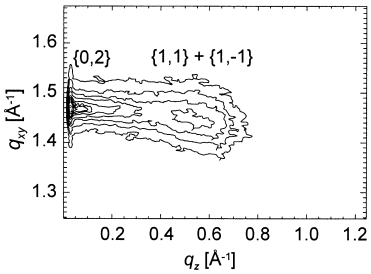

Figure 14. Two-dimensional contour plot of the scattered intensity $I(q_{xy}, q_z)$ from a monolayer of molecules of **5** at a nominal molecular area of 200 Å^2.

molecular area of 200 Å^2, displays two broad peaks that correspond to a centered, rectangular subcell of dimensions $a_s = 5.0$ Å, $b_s = 8.7$ Å. The molecules are tilted along the a_s axis by 25° with respect to the surface normal. These cell dimensions and the tilt direction of the chains appear now to be fingerprint evidence for the packing of all amphiphilic molecules containing the 1,3-bis(ethynylene)benzene unit as a spacer and which are aligned in ribbons parallel to the b_s axis. In this arrangement, the chains of one molecule are separated by an average distance of about 8.7 Å. Consequently, b_s is a subcell dimension and must be multiplied by four to give the true unit cell repeat as $b = 4\,b_s = 34.8$ Å. Along the a axis, the unit cell repeat is $a = a_s = 5.0$ Å. As this unit cell contains two molecules, each with four chains, the {0,2} and {1,1}+{1, – 1} Bragg peaks must be reassigned Miller indices of {0,8} and {1,4}+{1, – 4}, respectively. The molecular ribbons are stabilized by intermolecular van der Waals contacts with molecules in adjacent ribbons related by translation symmetry.

The crystalline film thickness of about 14 Å, as determined from the FWHM(q_z) of the two Bragg rods, indicates that chains with 12 – 13 CH_2 groups contribute to the diffraction signal. The two Bragg peaks in the GIXD pattern (Figure 14) partially overlap. The corresponding Bragg rods were separated by least-squares fitting the sum of two Gaussian profiles to the observed profile (Figure 15a), for X-ray structure factor calculations to be performed.

These computations, with the use of an atomic coordinate molecular model, yielded a good fit to the measured Bragg rods when chains of only 12 CH_2 groups were considered (Figure 15b,c). We interpret this result as indicating crystalline registry of only the central 12 CH_2 groups of the chains of the molecule **5**. The rest of the molecule does not contribute to the diffraction signal, because the regions close to the folds are not in registry. Figure 16a shows the packing arrangement

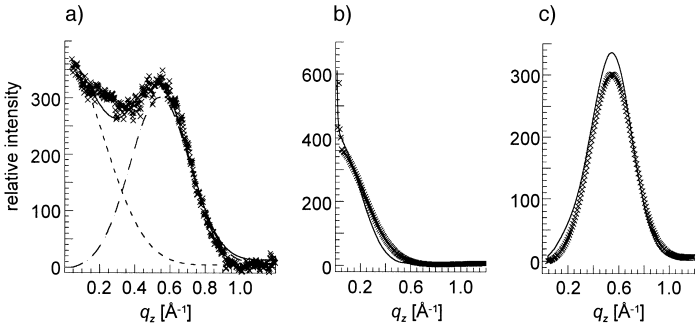

Figure 15. a) Separation of the measured Bragg rod intensity profile $I(q_z)$ (×) into two intensity profiles (dashed lines). b) and c): Measured (separated) (×) and calculated (line) intensity profiles $I(q_z)$ for the two Bragg rods, {0,8} and {1,4}+{1,−4}, assuming that chains of only 12 CH_2 groups contribute to the diffraction signal.

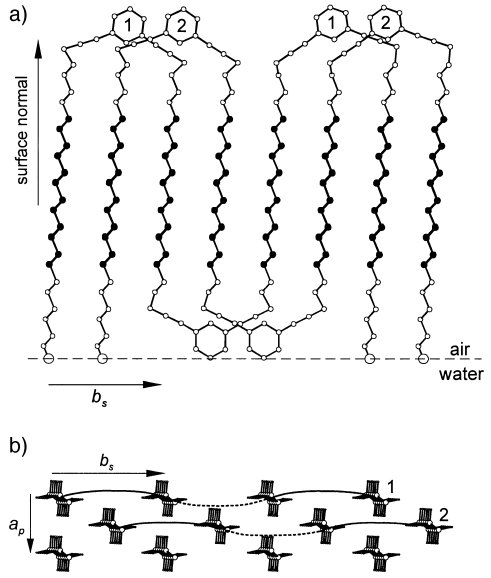

Figure 16. a) The atomic coordinate model of the chains of 12 CH_2 groups (full circles) superimposed on a molecular model of compound **5** (open circles) in the triply folded conformation viewed along the *a* axis. b) The two-dimensional crystalline packing arrangement of **5** viewed along the chain axis.

of the chains of 12 CH_2 groups superimposed on the molecular model of **5** in a triply folded conformation, as viewed along the *a* axis. In analogy to the monolayers of molecules **1** and **2**, those of **5** are arranged in molecular ribbons along the *b* axis (Figure 16b). The absence of reflections corresponding to the repeat spacings $0.5\,b$ and b indicates crystalline disorder, involving molecular ribbons parallel to b that may be randomly offset in steps of $\pm 0.25b$.

The crystalline coherence length, L, along the *a* axis, as determined from $L_{1,4} = 60$ Å, corresponds to about 24 molecular ribbons. We found $L_{0,8}$ to be 70 Å in the *b* direction; this corresponds to two molecules ($2\,b = 69.7$ Å) in registry. The GIXD pattern of this crystalline monolayer remains unchanged upon film compression to a nominal molecular area of 80 Å^2 (complete surface coverage).

In order to image the monolayer topography by SFM, films of compound **5** were transfered onto freshly cleaved mica by means of the horizontal-deposition technique. The SFM images shown in Figure 17 reveal different types of domain

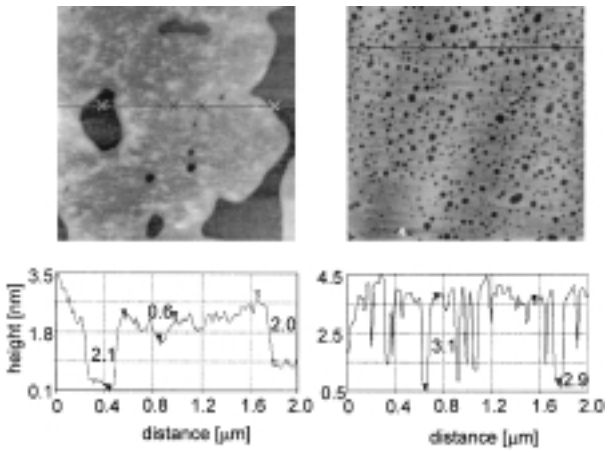

Figure 17. SFM topography images and height profiles of monolayers of molecule **5** transferred from the water surface onto freshly cleaved mica support; different domain morphologies are shown on the left and the right.

morphology, all with an average thickness of 20–30 Å. This value corresponds to a monolayer of compound **5** in the M-shape conformation. The surface roughness of about 6 Å is most likely caused by monolayer-surface disorder.

Conclusion

This work describes the use of the 1,3-bis(ethynylene)benzene unit for the induction of folding in oligomers at the air–water interface and to bring about self-assembled crystalline monolayers. This unit acts as a spacer, separating the stems of two linear alkyl chains in a molecule by about 9 Å. This distance is too large to allow intramolecular contacts between the relatively short chains during self-assembly, as observed for conventional two-chain amphiphiles such as **4** or phospholipids.[21, 31, 32] Nevertheless, a separation of 9 Å is twice the van der Waals distance between aliphatic chains in crystals. Therefore, only intermolecular van der Waals interactions can stabilize the molecules in a folded conformation in order to achieve close packing. Furthermore, the spacer unit confers good solubility in organic solvents, an essential requirement for the preparation of ordered monolayers on the water surface. The conformation and layer packing arrangement of this class of molecules was further confirmed by the three-dimensional crystal structure determination of a shorter analogue of molecule **2**, which contained chains of eleven carbon atoms.[33] Such a crystal is arranged as a centrosymmetric bilayer with two independent molecules within the layer; each molecule adopts the expected conformation and their chains are packed in a pseudo-herringbone motif.

Finally, our molecular design approach provides a tool for the preparation of polymers that would self-assemble into crystalline monolayers which expose a regular array of functional groups.

Experimental Section

Synthesis: The diiodobenzenes **6b** and **6c** were synthesized as previously described.[34a,b] The 1-alkynes **7a** and **7c** were obtained by a procedure

0947-6539/00/0612-2180 $ 17.50+.50/0 *Chem. Eur. J.* **2000**, *6*, No. 12

reported by Shaw,[35] with subsequent silylation.[36] All reactions were carried out under argon. For column chromatography, Merck silica gel (40–63 μm) was used. The abbreviation PE stands for petroleum ether with a boiling range of 30–40 °C. Diethyl ether and THF were freshly distilled from sodium/benzophenone. 1,3-Dimethyl-3,4,5,6-tetrahydro-2-pyrimidone (DMPU) was dried over CaH_2. NMR spectra were recorded on a BRUKER AMX300 at room temperature in $CDCl_3$, unless stated otherwise. The carbon multiplicity was determined with the DEPT experiment. Prior to elemental analysis and monolayer investigations, every sample was recrystallized from CH_2Cl_2 to remove dust particles or grease.

Compounds 1–3 and 9a: CuI (2 mol%) and $[Pd(PPh_3)_2Cl_2]$ (1 mol%) were added at room temperature to a degassed solution of 3,5-diiodobenzene (**6**) and 1-alkyne **7** (2.1 mol equiv) in THF (10 mL $mmol^{-1}$ of **6**) and piperidine (5 mL $mmol^{-1}$ of **6**). After being stirred for 16 h, the suspension was poured into diethyl ether, and the organic phase was washed with 2 N HCl. The combined aqueous phases were extracted with diethyl ether. The combined organic phases were washed with water and dried ($MgSO_4$), and the solvent was removed. Column chromatography (PE) followed by recrystallization in CH_2Cl_2 gave **3** (1.60 g, 78%) as a colorless solid.

Desilylation of crude **8a** and **8c** was carried out in THF with a solution of *n*-Bu_4NF in THF (1 M, 1 mol equiv relative to **7**, for 1 h at room temperature). After removal of the solvent in vacuo the residue was purified by column chromatography. The impurities were eluted with PE/diethyl ether (5:2 v/v). Subsequent elution with diethyl ether yielded **2** (0.19 g, 85%) and **9a** (3.05 g, 79%), respectively, as colorless solids.

Crude **8b** was deprotected by being stirred for 1 h in dioxane/MeOH/toluene sulfonic acid monohydrate (0.4 g, 2.1 mmol) at room temperature. Chromatography with PE/CH_2Cl_2 (2:1 v/v) led to the isolation of **1** (0.92 g, 80%) as a colorless solid.

Compound 1: ^{1}H NMR: $\delta = 0.86$ (t, $J = 6.7$ Hz, 6H), 1.15–1.48 (m, 76H), 1.48–1.63 (m, 4H), 2.35 (t, $J = 7.0$ Hz, 4H), 4.67 (br s, 1H), 6.74 (d, $J = 1.3$ Hz, 2H), 7.00 (t, $J = 1.3$ Hz, 1H); ^{13}C NMR: $\delta = 14.1$ (CH_3), 19.4, 22.7 ($2CH_2$), 28.7–29.7 (19 signals, CH_2), 79.7 (C), 91.0 (C), 117.8 (CH), 125.4 (C), 127.7 (CH), 155.0 (COH); elemental analysis calcd (%) for $C_{54}H_{94}O$ (759.346): C 85.41, H 12.48; found C 85.06, H 12.57.

Compound 2: ^{1}H NMR (35 °C): $\delta = 1.15$–1.48 (m, 76H), 1.48–1.63 (m, 8H), 2.36 (t, $J = 7.0$ Hz, 4H), 3.62 (t, $J = 6.6$ Hz, 4H), 7.13–7.18 (m, 1H), 7.24–7.27 (m, 2H), 7.40 (m, 1H);[36] ^{13}C NMR (35 °C): $\delta = 19.4$, 25.7 ($2CH_2$), 28.7–29.7 (19 signals, CH_2), 32.8, 63.1 ($2CH_2$), 80.0, 90.9, 124.2 (3C), 128.1, 130.5, 134.6 (3CH); elemental analysis calcd (%) for $C_{56}H_{98}O_2$ (803.400): C 83.72, H 12.30; found C 83.51, H 12.20.

Compound 3: ^{1}H NMR: $\delta = 0.86$ (t, $J = 6.7$ Hz, 6H), 1.15–1.48 (m, 76H), 1.56 (m, 4H), 2.24 (s, 3H), 2.35 (t, $J = 7.0$ Hz, 4H), 7.09 (br s, 2H), 7.21 (br t, 1H); ^{13}C NMR: $\delta = 14.1$ (CH_3), 19.4 (CH_2), 21.0 (CH_3), 22.7 (CH_2), 28.8–29.7 (18 signals, (CH_2)), 31.9 (CH_2), 80.1, 90.4, 124.0 (3C), 131.4, 131.7 (2CH), 137.8 (C); elemental analysis calcd (%) for $C_{55}H_{96}$ (757.373): C 87.22, H 12.78; found C 87.20, H 12.54.

Compound 9a: ^{1}H NMR (35 °C): $\delta = 1.15$–1.48 (m, 60H), 1.48–1.63 (m, 8H), 2.37 (t, $J = 7.0$ Hz, 4H), 3.62 (t, $J = 6.6$ Hz, 4H), 7.13–7.18 (m, 1H), 7.24–7.27 (m, 2H), 7.40 (m, 1H);[36] ^{13}C NMR (35 °C): $\delta = 19.4$, 25.8 ($2CH_2$), 28.7–29.7 (15 signals, CH_2), 32.9, 63.1 ($2CH_2$), 80.0, 90.9, 124.3 (3C), 128.1, 130.5, 134.6 (3CH); elemental analysis calcd (%) for $C_{48}H_{82}O_2$ (691.184): C 83.41, H 11.96; found C 83.35, H 12.02.

Synthesis of compound 5: Br_2 (0.66 mL, 12.9 mmol) was added at 0 °C to a solution of triphenylphosphine (3.37 g, 12.9 mmol) in CH_2Cl_2 (30 mL). After the reaction mixture was stirred for 30 min at room temperature, imidazole (0.92 g, 13.5 mmol) and **9a** (3.07 g, 4.4 mmol) were added. The resultant mixture was stirred for 4 h at room temperature. It was hydrolyzed with water, and the organic phase was washed with saturated aqueous $Na_2S_2O_3$, dried ($MgSO_4$), and concentrated in vacuo. The residue was purified by chromatography (PE/diethyl ether, 2:1 v/v) to give **9b** as a colorless solid (2.81 g, 78%).

n-BuLi in *n*-hexane (1.6 M, 4.32 mL, 6.91 mmol) was slowly added to a solution of trimethylsilylacetylene (0.74 g, 7.53 mmol) in THF (20 mL) at −80 °C. After addition of DMPU (20 mL) and **9b** (2.57 g, 3.14 mmol), the temperature was allowed to rise slowly to room temperature. Stirring for 16 h at room temperature, aqueous workup, followed by drying ($MgSO_4$), deprotection in THF with *n*-Bu_4NF (5.5 mL, 1 M solution in THF), removal of the solvent in vacuo, and subsequent column chromatography (PE/dichloromethane, 7/1 v/v) gave **9c** (1.62 g, 80%) as a colorless solid.

The procedure for the aryl–alkyne coupling reaction as described for compounds **8a–c** and **3** was followed for the coupling of 1,3-diiodobenzene (**6a**, 3.90 g, 11.8 mmol) with **7b** (5.00 g, 11.8 mmol) to give, after column chromatography (PE/diethyl ether, 5/1 v/v), compound **10** (5.54 g, 75%) as a colorless solid.

The procedure for the aryl–alkyne coupling reaction as described for compounds **8a–c** and **3** was followed for the coupling of **9c** (0.35 g, 0.5 mmol) with **10** (0.67 g, 1.0 mmol) to give, after chromatography (PE, PE:CH_2Cl_2 = 70:9 v/v, PE:diethyl ether = 5:2 v/v), the silylated compound **5** (0.6 g, 67%). Part of this material (0.28 g) was desilylated in THF with *n*-$BuNF_4$ (0.5 mL, 1 M solution in THF). Removal of the solvent, followed by chromatography (diethyl ether) yielded **5** (0.19 g, 68%) as a colorless solid.

Compound 9b: ^{1}H NMR: $\delta = 1.15$–1.48 (m, 60H), 1.57 (m, 4H), 1.83 (m, 4H), 2.36 (t, $J = 7.0$ Hz, 4H), 3.39 (t, $J = 6.9$ Hz, 4H), 7.13–7.18 (m, 1H), 7.24–7.27 (m, 2H), 7.40 (m, 1H);[37] ^{13}C NMR: $\delta = 19.4$, 28.2 ($2CH_2$), 28.7–29.7 (15 signals, CH_2), 32.9, 34.0 ($2CH_2$), 80.0, 90.9, 124.2 (3C), 128.1, 130.5, 134.6 (3CH); elemental analysis calcd (%) for $C_{48}H_{80}Br_2$ (816.968): C 70.57, H 9.87; found C 70.21, H 9.98.

Compound 9c: ^{1}H NMR: $\delta = 1.15$–1.48 (m, 60H), 1.48–1.63 (m, 8H), 1.92 (t, $J = 2.6$ Hz, 2H), 2.16 (dt, $J_d = 2.6$ Hz, $J_t = 7.0$ Hz, 4H), 2.36 (t, $J = 7.0$ Hz, 4H), 7.13–7.18 (m, 1H), 7.24–7.27 (m, 2H), 7.40 (m, 1H);[37] ^{13}C NMR: $\delta =$ 18.4, 19.4, 28.5 ($3CH_2$), 28.7–29.7 (16 signals, CH_2), 68.0 (CH), 80.0 (C), 84.8 (C), 90.8 (C), 124.2 (C), 128.1, 130.5, 134.6 (3CH);[38] elemental analysis calcd (%) for $C_{52}H_{82}$ (707.228): C 88.31, H 11.69; found C 88.41, H 11.71.

Compound 10: ^{1}H NMR: $\delta = 0.03$ (s, 6H), 0.88 (s, 9H), 1.15–1.63 (m, 42H), 2.36 (t, $J = 7.0$ Hz, 2H), 3.58 (t, $J = 6.6$ Hz, 2H), 6.98 (t, $J = 7.8$ Hz, 1H), 7.31 (td, $J_t = 1.6$ Hz, $J_d = 7.8$ Hz, 1H), 7.56 (td, $J_t = 1.6$ Hz, $J_d = 7.8$ Hz, 1H), 7.73 (t, $J = 1.6$ Hz, 1H); ^{13}C NMR: $\delta = -5.3$ (CH_3Si), 18.4 (C), 19.4, 25.8 ($2CH_2$), 26.0 (CH_3), 28.6–29.7 (19 signals, CH_2), 32.9, 63.3 ($2CH_2$), 79.0 and 92.1 (2 C), 93.6 (CI), 126.3 (C), 129.6, 130.7, 136.5,140.2 (4CH); elemental analysis calcd (%) for $C_{37}H_{65}OISi$ (680.917): C 65.27, H 9.62; found C 65.38, H 9.62.

Compound 5: ^{1}H NMR (35 °C): $\delta = 1.15$–1.35 (m, 138H), 1.48–1.63 (m, 16H), 2.36 (t, $J = 7.0$ Hz, 12H), 3.62 (t, $J = 6.6$ Hz, 4H), 7.13–7.18 (m, 1H), 7.24–7.27 (m, 2H), 7.40 (m, 1H);[36] ^{13}C NMR (35 °C): $\delta = 19.4$, 25.8 ($2CH_2$), 28.7–29.7 (20 signals, CH_2), 63.1 (CH_2), 80.0, 90.9, 124.3 (3C), 128.1, 130.5, 134.6 (3CH); elemental analysis calcd (%) for $C_{114}H_{182}O_2$ (1584.710): C 86.40, H 11.58; found C 86.07, H 11.54.

Synthesis of compound 4: Docosyl bromide (4.58 g, 11.8 mmol) was slowly added to Mg (0.34 g, 14.1 mmol) in diethyl ether (30 mL). After being refluxed for 16 h, docosyl magnesium bromide **12** was added to a solution of **11** (1.25 g, 4.5 mmol) and $[Ni(dppp)Cl_2]$ (0.025 g, 0.045 mmol) in diethyl ether (20 mL). After being refluxed for 5 days, the reaction mixture was poured onto ice. The organic phase was washed with 2 N HCl. The aqueous phase was extracted with diethyl ether. The combined organic phases were washed with saturated aqueous Na_2CO_3 and dried ($MgSO_4$), to give crude, *O*-silylated **4**. Deprotection in THF with *n*-$BuNF_4$ (2.5 mL, 1 M solution in THF) for 2 h at room temperature, and subsequent column chromatography, elution first with PE/dichloromethane (7:1 v/v), then with PE/diethyl ether (1:1 v/v), yielded compound **4** (1.80 g, 56%) as a colorless solid.

Compound 4: ^{1}H NMR: $\delta = 0.87$ (t, $J = 6.7$ Hz, 6H), 1.15–1.40 (m, 76H), 1.50–1.65 (m, 4H), 2.50 (t, $J = 7.7$ Hz, 4H), 4.48 (s, 1H), 6.45 (br d, $J = 1.1$ Hz, 2H), 6.56 (br t, 1H); ^{13}C NMR: $\delta = 14.1$ (CH_3), 22.7 (CH_2), 29.4–29.7 (17 signals, CH_2), 31.3, 31.9, 35.9 ($3CH_2$), 112.5, 121.3 (2CH), 144.6, 155.4 (2C); elemental analysis calcd (%) for $C_{50}H_{94}O$ (711.302): C 84.43, H 13.32; found C 84.30, H 13.40.

***Π*–*A* isotherms**: The surface-pressure–area (–*A*) isotherms were measured with a computer-controlled Lauda film balance placed in a laminar hood. The sample solutions in $CHCl_3$ (2.5–6.0×10^{-4} M) were spread on the water subphase at 20 °C and the system was allowed to equilibrate for 30 min at 5 °C. The water used had been purified by a Millipore purification system to give a resistance of 18 MΩ cm.

SFM measurements: For SFM measurements, the monolayers were transferred onto freshly cleaved mica by the horizontal-deposition technique. The mica pieces (1 × 1 cm) were placed on a stainless steel mesh inside a specially designed teflon trough.[39] The trough was filled with water and the sample solutions were spread on the water surface at 20 °C.

After the system was equilibrated for 30 min at 5 °C, the resulting Langmuir monolayers were deposited on the mica by slow removal of the water with a motor-driven syringe. After the samples were dried in air, the SFM measurements were carried out with a Topometrix TMX 2010 stage with integrated Si_3N_4 pyramidal tips on cantilevers, with force constants between 0.03 – 0.40 N m^{-1}. The applied contact force during imaging exceeded the equilibrium force by 2 – 5 nN and had been recorded before the contact was made.

GIXD measurements: Grazing incidence X-ray diffraction (GIXD), a surface-sensitive, in situ analytical method for the investigation of Langmuir monolayers, is described in detail elsewhere.[20] The GIXD experiments were carried out at the beamline BW1 with the liquid surface diffractometer at Hasylab synchrotron source, DESY, Hamburg. The sample solutions ($2.5 - 6.0 \times 10^{-4}$ M) were spread on the water subphase at 20 °C. The trough, mounted on the diffractometer and equipped with a Wilhelmy balance, was sealed, flushed with helium, and equilibrated at 5 °C for 1 h. A monochromatic X-ray beam was adjusted to strike the water surface at an incident angle $\alpha_i \approx 0.85\alpha_c$ (where α_c is the critical angle for total external reflection of X-rays for the air – water interface). The dimensions of the footprint of the incoming X-ray beam on the water surface are approximately 2×50 or 5×50 mm^2. The measurements were performed by scanning over a range along the horizontal component of the X-ray scattering vector, $q_{xy} \approx (4\pi/\lambda)\sin(2\theta_{xy}/2)$, in which $2\theta_{xy}$ is the angle between the projections onto the horizontal plane of the incident and the diffracted beams. The scattered intensity was detected by a position-sensitive detector (PSD), which resolves the vertical component of the X-ray scattering vector, $q_z \approx (2\pi/\lambda)\sin\alpha_f$ (where α_f is the vertical angle between the diffracted beam and the horizon), in the q_z range 0.00 to 1.40 Å^{-1}. The diffraction data may be presented in three ways: i) the GIXD pattern as a two-dimensional intensity distribution $I(q_{xy}, q_z)$ in a surface or contour plot; ii) the GIXD pattern $I(q_{xy})$ obtained by integrating over the whole q_z window of the PSD, which yields the Bragg peaks; iii) the Bragg rod intensity profiles, which are the scattered intensity $I(q_z)$ recorded in channels along the PSD integrated across the q_{xy} range of each Bragg peak. Several different types of information were extracted from the measured GIXD pattern. The $2\theta_{xy}$ (or q_{xy}) positions of the Bragg peaks are used for the calculation of the lattice repeat distances $d = 2\pi/q_{xy}$, and when these are assigned {*h*,*k*} Miller indices, the unit cell parameters *a* and *b* are obtained. The vertical full width at half maximum, FWHM(q_z), of the Bragg rod intensity profiles gives an estimate of the thickness: $d \approx 0.9(2\pi/\mathrm{FWHM}(q_z))$ of the crystalline film on the water surface. The horizontal full width at half maximum of the Bragg peaks FWHM(q_{xy}) yields the crystalline coherence lengths $L_{hk} \approx 0.9(2\pi/\mathrm{FWHM}(q_{xy}))$. For long, linear molecules (or for the more complicated molecules that consist mainly of long, straight, parallel hydrocarbon segments), to a first approximation, the tilt angle *t* of the molecular axis with respect to the normal to the interface and the horizontal azimuthal direction of the tilt can be determined[40] from the set of equations: $\cos\psi_{hk}\tan t = q_{z,max}/|(\boldsymbol{q}_{hk})|$, in which, for each (*h*,*k*) Bragg rod, ψ_{hk} is the azimuthal angle between the molecular tilt direction projected onto the *xy* plane and the reciprocal lattice vector $\boldsymbol{q}_{hk}$ and $q_{z,max}$ is the peak position along the Bragg rod. For more quantitative purposes, the intensity at each q_z value in a Bragg rod intensity profile is of course given by the square of the molecular structure factor $F_{hk}(q_z)$. Thus, X-ray structure factor calculations were performed with the use of atomic coordinate models, to yield $I(q_z)$ values that fit the measured Bragg rod intensity profiles.[24]

Specular X-ray reflectivity:[20] Specular X-ray reflectivity measurements of a film at the air – water interface may be inverted to give the vertical density profile across the interface; this profile is laterally averaged over all of the film and not just the crystalline part of it. The information gained includes the thickness and the surface roughness of the film. The measurements were carried out with the same liquid-surface diffractometer used for the GIXD experiments. The X-ray reflectivity was performed on the film of molecule **3** at a nominal molecular area of 50 Å^2 by scanning the incident beam angle α_i (equal to the reflected beam angle α_r) from $0.5\alpha_c$ to $42\alpha_c$. The reflected radiation was measured by a NaI scintillation counter. The measured reflectivity is presented in the form of normalized X-ray reflectivity R/R_F (R_F is the Fresnel reflectivity calculated for a perfect, sharp interface) as a function of the normalized vertical scattering vector q_z/q_c, where $q_z = (4\pi/\lambda)\sin\alpha_r$ and q_c is the scattering vector at the critical angle of incidence α_c, $q_c = (4\pi/\lambda)\sin\alpha_c$.

Acknowledgements

We thank Dr. S. Cohen for the SFM measurements and Dr. S. Höger for supplying the starting material **6c**. We are grateful to HASYLAB at DESY, Hamburg, Germany for beam time. We thank the German Israeli Foundation, the G. M. J. Schmidt Minerva Centre of Supramolecular Architectures, the Danish Foundation for Natural Sciences (DanSync programme), and the European Community (TMR-Contract ERBFMGECT950059) for their support.

[1] J. A. McNew, J. M. Goodman, *Trends Biochem. Sci.* **1996**, *21*, 54 – 58.
[2] V. A. Ogarev, *Colloid J.* **1997**, *59*, 625.
[3] A. Keller, *Macromol. Symp.* **1995**, *98*, 1.
[4] G. Ungar, J. Stejny, A. Keller, I. Bidd, M. C. Whiting, *Science* **1985**, *229*, 386.
[5] T. Yamamoto, *J. Chem. Phys.* **1997**, *107*, 2653.
[6] P. R. Sundararajan, T. A. Kavassalis, *J. Chem. Soc. Faraday Trans.* **1995**, *91*, 2541.
[7] T. A. Kavassalis, P. R. Sundararajan, *Macromolecules* **1993**, *26*, 4144.
[8] S. J. Sutton, A. S. Vaughan, D. C. Basset, *Polymer* **1996**, *37*, 5735.
[9] D. C. Basset, R. H. Olley, S. J. Sutton, A. S. Vaughan, *Polymer* **1996**, *37*, 4993.
[10] S. J. Organ, G. Ungar, A. Keller, *Macromolecules* **1989**, *22*, 1995.
[11] G. Ungar, *Polymer* **1986**, *27*, 1835.
[12] G. L. Gaines, *Insoluble Monolayers at Liquid – Gas Interfaces*, Interscience, New York, **1966**.
[13] S. P. Weinbach, I. Weissbuch, K. Kjaer, W. G. Bouwman, J. Als-Nielsen, M. Lahav, L. Leiserowitz, *Adv. Mater.* **1995**, *7*, 857.
[14] D. Jaquemain, F. Leveiller, S. P. Weinbach, M. Lahav, L. Leiserowitz, K. Kjaer, J. Als-Nielsen, *J. Am. Chem. Soc.* **1991**, *113*, 7684.
[15] I. Weissbuch, R. Popovitz-Biro, M. Lahav, L. Leiserowitz, *Acta Crystallogr.* **1995**, *51*, 115.
[16] R. Popovitz-Biro, R. Edgar, I. Weissbuch, R. Lavie, S. Cohen, K. Kjaer, J. Als-Nielsen, E. Wassermann, L. Leiserowitz, M. Lahav, *Acta Polym.* **1998**, *49*, 626.
[17] I. Weissbuch, K. Lederer, A. Godt, K. Kjaer, J. Als-Nielsen, P. B. Howes, G. Wegner, M. Lahav, L. Leiserowitz, *J. Phys. Chem. B* **1998**, *102*, 6313.
[18] I. Weissbuch, R. Popovitz-Biro, M. Lahav, L. Leiserowitz, K. Kjaer, J. Als-Nielsen, *Adv. Chem. Phys.* **1997**, *102*, 39.
[19] D. Jaquemain. S. G. Wolf. F. Leveiller, M. Deutsch, K. Kjaer, J. Als-Nielsen, M. Lahav, L. Leiserowitz, *Angew. Chem.* **1992**, *104*, 134; *Angew. Chem. Int. Ed. Engl.* **1992**, *31*, 130.
[20] J. Als-Nielsen, D. Jaquemain, K. Kjaer, F. Leveiller, M. Lahav, L. Leiserowitz, *Phys. Rep.* **1994**, *246*, 251.
[21] C. A. Helm, H. Möhwald, K. Kjaer, J. Als-Nielsen, *Biophys. J.* **1987**, *52*, 381.
[22] S. Takahashi, Y. Kuroyama, K. Sonogashira, N. Hagihara, *Synthesis* **1980**, 627.
[23] M. Kumada, K. Tamao, K. Sumitani, *Org. Synth.* **1978**, *58*, 127.
[24] F. Leveiller, D. Jaquemain, L. Leiserowitz, K. Kjaer, J. Als-Nielsen, *J. Phys. Chem.* **1992**, *96*, 10380.
[25] CERIUS^2, molecular modeling software for materials research from BIOSYM/Molecular Simulations, San Diego CA (USA) and Cambridge (UK).
[26] We did not measure the very low q_{xy} region corresponding to the {01} Bragg rod.
[27] A. W. Adamson, *Physical Chemistry of Surfaces*, Wiley, New York, **1990**, p. 69.
[28] A. I. Kitaigorodskij, *Organic Chemical Crystallography*, Consultants Bureau, New York, **1961**, p. 117.
[29] Note that this peak corresponds to a *d* spacing of 4.7 Å. Since other new peaks were not encountered, we cannot assign this phase.
[30] K. Kjaer, W. G. Bouwman, *Hasylab Annual Report* **1994**, p. 405.
[31] K. Kjaer, J. Als-Nielsen, C. A. Helm, L. A. Laxhuber, H. Möhwald, *Phys. Rev. Lett.* **1987**, *58*, 2224.
[32] C. A. Helm, H. Möhwald, K. Kjaer, J. Als-Nielsen, *Europhys. Lett.* **1987**, *4*, 697.
[33] K. Lederer, V. Enkelmann, unpublished results.

  0947-6539/00/0612-2182 $ 17.50+.50/0

[34] a) **6b**: S. Höger, K. Bonrad, unpublished results; **6c**: b) H. L. Wheeler, L. M. Liddle, *Am. Chem. J.* **1909**, *42*, 441.
[35] Preparation analogously to the procedure given by S. R. Abrams, A. C. Shaw, *Org. Synth.* **1987**, *66*, 127.
[36] E. J. Corey, A. Venkateswarlu, *J. Am. Chem. Soc.* **1972**, *94*, 6190.
[37] Spectrum of higher order; H. Friebolin, *Ein- und Zweidimensionale NMR-Spektroskopie*, VCH, Weinheim, **1988**, p. 92.
[38] The C atom multiplicity of these two signals could not be determined unambiguously on the basis of the DEPT 135 spectrum. Assignment according to: H. O. Kalinowski, S. Berger, S. Braun, *13C-NMR-Spektroskopie*, Thieme, Stuttgart, **1984**, chapter 3, p. 130.
[39] J. Majewski, L. Margulis, I. Weissbuch, R. Popovitz-Biro, T. Arad, Y. Talmon, M. Lahav, L. Leiserowitz, *Adv. Mater.* **1995**, *7*, 26.
[40] K. Kjaer, *Physica B*, **1994**, *198*, 100.

Received: October 1, 1999 [F2064]

  0947-6539/00/0612-2183 $ 17.50+.50/0